IJE TRANSACTIONS B: Applications Vol. 37, No. 05, (May 2024) 920-930

International Journal of Engineering

Journal Homepage: www.ije.ir

Heat Transfer Augmentation for Impingement of Steady Air Jet under Exponential Heat Flux Boundary Condition

A. M. Rathod[a], N. P. Gulhane[a], U. M. Siddique*[b]

[a] *Department of Mechanical Engineering, Veermata Jijabai Technological Institute, Mumbai, India*
[b] *Department of Production Engineering, Veermata Jijabai Technological Institute, Mumbai, India*

PAPER INFO

Paper history:
Received 15 September 2023
Received in revised form 14 November 2023
Accepted 13 December 2023

Keywords:
Nusselt Number
Exponential Varying Heat Flux
Cooling Rate
Slope
Heat Transfer

ABSTRACT

The cooling rate under impingement of air jet finds massive application in electronic packaging, material processing industries and cooling of gas turbine. The conventional cooling of heat sinks was till date carried out using a fan and pump. Recently, the momentous impingement of air has been found to produced 1.5 times the cooling rate, as compared with conventional method, under same pumping power. Previously, attractive amount of Research is carried out in observing the cooling rate for constant heat flux boundary condition, and less are available for constant wall temperature. The present research provides an in-depth numerical investigation for such jet impinged heat sinks, with a heat flux boundary condition. The exponential variation of heat flux magnitude with radial distance (Away from impingement point), is observed to be a generic alternate of constant wall temperature boundary condition. The numerical computation for heat transfer of such exponentially powered heat flux sink is carried out using FLUENT (ANSYS 2023R1). An orthogonal 2-D mesh computational domain with a compactible SST and K-Omega turbulence model is simulated for various inlet velocity and nozzle-target spacing. The impingement of jet and local cooling of target surface is defined using a well know non-dimensional Reynolds and Nusselt number, respectively. The exponential power for non-uniformly heated sinks can be readily selected (0.1-1) to replicate the present non-uniform heating or constant wall temperature boundary condition. Non-uniform heating has gained lots of attention of heat transfer researcher across the globe. The computation results extracted for various impinging Reynolds number and nozzle-target spacing, were closely best fitted using regression and validated with referred previous literature results. Tight dependency of slope parameter, over Reynolds number and z/d is observed in local cooling rate. These dependencies are judged based on the power of exponents. The semi – empirical correlations are defined separately for and stagnation, transition, and wall jet regions, separately. Such correlation can plan the design of cooling system, under non-uniform heating conditions

doi: *10.5829/ije.2024.37.05b.10*

Graphical Abstract

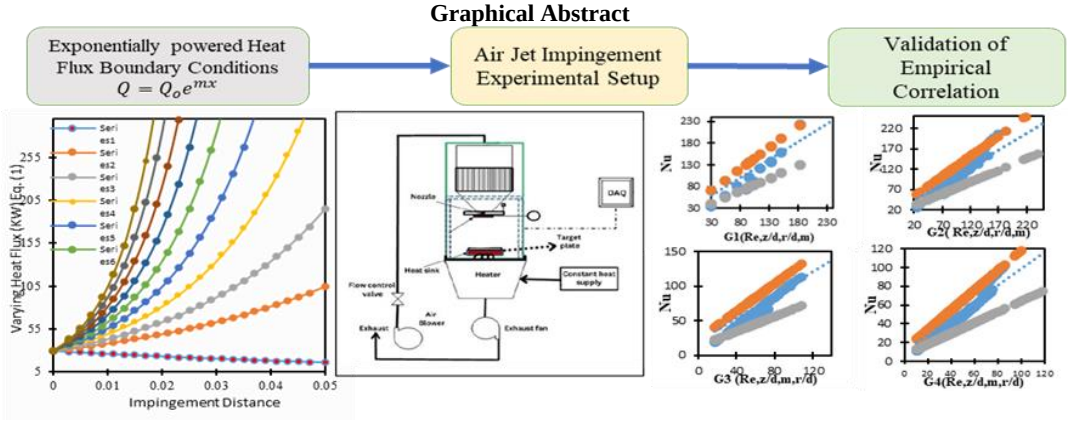

*Corresponding Author Email: u.i.siddiqui@gmail.com (U. M. Siddique)

Please cite this article as: Rathod AM, Gulhane NP, Siddique UM, Heat Transfer Augmentation for Impingement of Steady Air Jet under Exponential Heat Flux Boundary Condition. International Journal of Engineering, Transactions B: Applications. 2024;37(05):920-30.

NOMENCLATURE

Re	Reynolds number	m	The slope of heat flux	$G1, G2, G3$ &$G4$	Functions
Pr	Prandtl number	Nu	Nusselt number	**Greek Symbols**	
GR	Growth rate	ΔT	Temperature difference	P	Density of air
z	Nozzle exit to target surface spacing	z/d	Nozzle target spacing	α	Thermal Diffuisvity
h	Heat transfer coefficient	C	Non-dimensional constant	ω	Specific Dissipation rate
Q and Q_o	Heat flux (w/m^2)	t	Geometric thickness	μ	Dynamic viscosity
$\overline{T_s}$	Average surface temperature	$\overline{T_f}$	Mean Bulk Fluid Temperature	C_p	Specific heat

1. INTRODUCTION

The continuous demand in cooling rate for efficient working of work station, electronic packaging system and material processing industries, is continuously being investigated by heat transfer researcher and postdoc. The conventional method of cooling using fan immensely demands for higher pumping power, increasing the running cost of system. Jet impingement using heat transfer, resulting in around 150% increase in cooling rate with same pumping power, was observed in early 1990's. Till date the steady jet impingement heat transfer is almost completely investigated and sufficient empirical correlations are readily available for design of cooling system. The air jet impingement over a hot target surface is a study partially in line with external force convection. Ricou et al. (1) for the first time investigated the entrainment effect of atmospheric air in suppressing the overall cooling rate for a fully developed laminar impingement. The Nusselt profile $\left(Nu\ vs\frac{r}{d}\right)$ for the isothermal impinging jet was found to have the same velocity gradient over target surface as that of the one with higher/ lower temperature as that of target surface. The fully developed turbulent impingement is more of mixed convection and very less ($\pm 2\%$) natural convection (1). Hoogendoorn (2) investigated the heat transfer near stagnation zone, using liquid crystal technique. It was observed for the nozzle target spacing $\left(\frac{z}{d} > 5\right)$ the stagnant point heat transfer is equivalent to that of the flow past the cylinder, provided the cylinder is five times the diameter as that of target surface. The fully developed turbulent impingement is majorly observed to possess a turbulence intensity greater than 1%. The turbulence intensity is the measure of root mean square velocity at nozzle exit. Pamadi and Belov (3) observed the secondary peak in the Nusselt profile near transition and far jet region (r/d >2.5). Such peaks are more prone to happen with lower nozzle target spacing $\left(\frac{z}{d} < 1\right)$ (4). Using finite difference technique of Kolmogorov-Prandtl hypothesis, secondary peaks were even bound to observed in stagnation zone due to some turbulence palpitation. Kataoka (5) observed the fluid density variation for free jets of burned gas and $CO2$ air mixture. The potential core of impinging jet as observed by Behera et al. (6), is the core length of velocity at nozzle exits. This core of impinging jet is least affected by entrainment effect and has poor cross diffusion of momentum. The potential core of temperature development was correlated with inlet temperature by Behera (6). A generalize model for logarithmic mean temperature difference in terms of core length conveys an exponential decay in Nusselt profile with respect to radial distance. The radial distance is measured from the point of impingement to the extreme of target surface. Shadlesky (7) investigated the existence of critical range of Stanton number for fully developed potential core of impinging jet. The developed potential core is highly sensitive to the nature of development of velocity at nozzle exit. Between 0.57 and 0.763 (St), the flow exit the nozzle carries a fully developed potential core. With a temperature difference $0℃ < \Delta T < 60℃$, an overall difference of $15\% - 25$ % was observed with overall cooling rate proposed by Hollworth and Gero (8), the Nusselt number magnitude empirical correlation as summation of heat transfer due to turbulence and heat transfer due to temperature difference as, $q_s = h\Delta T_1 + h\emptyset\Delta T$. The heat transfer due to turbulence is majorly due to adverse pressure gradient at the point of impingement. Zumbrunnen et al. (9) investigated the transient heat transfer cooling rate for pulse impingement air jet. The data points were recorded for before and after the renewal/vanish of thermal boundary layer. Empirical relation for water jet impingement $(Nu_{wt} = Re_w^m . Pr^{0.4}, 60 - 90\%)$ at stagnation point was found to independent of pulse rate. Major enhancements were attributed to the turbulence jet intensity and vorticity amplification. A 25% uncertainty with turbulent impingement and 11% for laminar was observe by Zumbrunnen et al. (9). Goldstein and Seol (10) investigated the average cooling rate for the row of impinging circular and square shape jet, with a fully developed velocity profile at outlet of nozzle. The $\frac{Nu}{Re^{0.7}}$ against the span wise position of target surface under constant heat flux was investigated for $1 < \frac{z}{d} < 6$ and $10000 < Re < 25000$. The cooling rate at stagnation region was found to dominate over the other local position. In line with the previous literature, less significant change in Nusselt profile and overall cooling rate for variation in span wise distribution spacing of nozzle $\left(1 < \frac{s}{d} < 4\right)$, was observed. This is due to the poor mixing of potential core of consecutive impinging jet. The research work concluded the higher area averaged cooling rate for closely spaced impinging

nozzle. The premixing of potential core of optimally spaced nozzle induces higher turbulence over the target surface. With nozzle target spacing less than 1. Lytle and Webb (11) observed a significant increase in stagnant point heat transfer and few secondary peaks. These secondary peaks observed in $\left(1 < \frac{r}{d} < 2.5\right)$, is the recovery effect for the continuity equation. The secondary peaks $\left(\frac{z}{d} > 1\right)$ shifts radially out with increase in Reynolds number from 5100 to 23000. Behnia (12) reported the computational results for $v^2 - f$ turbulence model for predicting the flow over the target surface for a confined impingement of jet. This enhancement due to the confinement of jet was observed for $30000 < Re < 70000$. The degree of confinement is determined with the premixing of potential core of impinging jet with atmospheric air. Garimella and Schroeder (13) investigated the impingement of multi-jet and its effect on overall cooling rate. With $2 \times 2$and 6×6 sets of impinging nozzles, the stagnant heat transfer secondary peaks were observed distinguished for $(\frac{s}{d} > 4)$ (9). Up till, here it can be well concluded that utilization of pumping power of impinging jet in the form of heat transfer is much challenging for single jet. The impingement of multi-jet reflects some secondary peaks to dissolve its pumping power, through some turbulence mixing. The present study proposed few such empirical correlation of $Nu = f_1\left(Re, \frac{z}{d}, \frac{r}{d}\right)$. Han and Goldstein (14) gave a summary review of crossflow diffusion and angle of impingement against the overall cooling rate. With impingement angle of 90^o, the Nusselt profile against the radial distance was observed to be perfectly symmetrical (mirror image). Not much deviation in overall cooling rate $(10\% - 25\%)$ with variation in angle of impingement was observed. Katti and Prabhu (4) investigated local heat transfer distribution between a smooth flat surface and impinging of air from a circular straight pipe nozzle. Three vital heat transfer region were observed, stagnation $\left(\frac{r}{d} = 0\right)$, transition $\left(1 < \frac{r}{d} < 2.5\right)$ and wall jet $\left(\frac{r}{d} > 2.5\right)$ for fully developed impingement. The local heat transfer characteristics were estimated for varying Reynolds numbers between 12000 and 28000 and nozzle-target spacing of 0.5 - 8 nozzle diameters. Sagot et al. (15) validated the SST K-omega turbulence model for the impingement of gas at a temperature greater than that of the target surface, demonstrating the heating application of impingement heat transfer. Good validation with Dittus-Boelter equation with $Pr^{0.4}$ was observed, Sagot et al. (15) reported the robustness of SST K-omega in predicting the heat transfer rate within $\pm 10\%$ uncertainty with general equation of internal forced convection (16). Alimohammadi et al. (17) numerically predicted the local heat transfer coefficients of an unconfined steady impinging air jet with a constant temperature boundary condition. The secondary peak was observed by coupling the SST turbulence model with Gamma-Theta transition model. Maximum of 5% deviation in local, area-averaged and stagnation Nusselt number for $\frac{H}{D} = 1$ and $Re = 14000$ was observed. Guo et al. (18) investigated the transient heat transfer due to the impingement of a $6mm$ diameter circular jet and reported the event of steadiness in cooling, after 80s of start of impingement. The numerical validation of an ICEM-CFD-3D meshed computational domain was computed with fluent solver to observe the velocity contour at different time step (before 80s). The numerical work was validated against the experimental results within $\pm 10\%$ accuracy of Nusselt number, with previous literature work. The author reported a significant increase in cooling rate with increase in nozzle target spacing $(4 < \frac{z}{d} < 8.5)$ for the jet impinging at $Re = 34000$. Luhar et al. (19) reported the set of algebraic equation used in determining temperature coefficients and proposed analytical model. This analytical model was constructed using finite different scheme. Sundaram and Venkatesan (20) studied heat transfer characteristics over the pin fin surface using RNG Turbulence model. It was observed that temperature decreases with the number of perforation of pin. Umair and Gulhane (21) observed Nusselt profile variation with the emergence of secondary peaks at lower nozzle target spacing $(\frac{r}{d} < 1)$.

These variations were attributed to the presence of turbulence flow near stagnation region. In line with the previous literature, Umar et al. (22) proposed semi empirical correlation with low nozzle target spacing $\left(\frac{r}{d} < 1\right)$. These correlation established a power law relation across four specific regions: stagnation, near wall, far wall and jet region. Umair and Gulhane (23) reported the non-uniformity in cooling characteristics of target surface. Thermal diffusivity (property variation) and geometric thickness (target surface) were studied for the occurrences of unevenness in Nusselt profile. The author reported a critical dependency of non-uniformity (Nusselt Profile) for air flow rate, below $59.33 - 66.76\ mm^3/s$. Siddique et al. (24) also investigated the effect of target surface thickness in inducing the un evenness to the profile cooling. Well clarified semi empirical correlation for $Pr \times \frac{t}{d} < 0.012$ and $Pr \times \frac{t}{d} < 0.012$ was reported. The work future recommended the existence of the Nusselt number correlation as function of $Pr, \frac{t}{d}, \frac{z}{d}, Re$ & $\frac{r}{d}$, which take care of such non-uniformity/ unevenness. Umair et al. (23) experimental readings were validated with the coupled SST and Gamma – theta transition model in CFX. The Standard deviation in Nusselt profile converge with the increase in the value of constant $c = \frac{Re}{z/d} > 6000$. Recently, Siddique

et al. (25) numerically investigated the modification in transitional semi empirical correlation of Nusselt number with linearly varying heat flux. The article carried the numerical work with unevenness in Nusselt profile, considering the slope parameter (m). Husain and Ariz (26) studied the effect of design parameter using 3D computational model to enhance heat transfer with effusion holes. Aminzadeh et al. (27) numerically examined the impact of inlet flow rate and temperature differences (0, 100, and 300K) on the behavior of a self-excited oscillating jet with Reynolds number 1000 and 3000. $\pm 10\%$ deviation in overall cooling rate was observed. The effect of viscous dissipation on heat transfer coefficient in laminar, non-Newtonian flows studied by Manglik and Prusa (28). The Nusselt number correlation with wall temperature gradient in transition region was proposed. Lu and Cheng (29) analyzed the friction factor and Nusselt number for viscous compressible flow in a tube. The turbulence friction factor was observed to be a strong function of velocity gradient and varies with impinging temperature. Wang et al. (30) experimentally investigated forced convection over NACA-63421 airfoil, for different temperature of streamed impinging jet, ranging from $-30\,℃\ to\ 20℃$. At $Re \geq 5 \times 10^5$, the average Nusselt number fluctuation was observed to be greater for a cylinder a compared with flat plate airfoil. The value of Nusselt density varying Reynold number $\left(0\ to\ 2\frac{g}{m^3}\right)$ for multiphase flow was proposed in terms of local Nusselt number. The uncertainty of Nusselt number was observed to lie within 7.34 %. Wang et al. (31) proposed a new non-dimensional correlation of heat transfer coefficient with impinging droplet on NACA airfoil at different angle of attack. The present work is actually inclined with a non – uniform heat flux boundary condition, and the degree of local unevenness is considered using a slope parameter (m). The average and local Nusselt number were found to vary with angle of attack. Extensive and massive work is carried out for predicting the externa flow heat transfer coefficient (Nusselt number) for impinging jet and sufficient correlations are available in terms of Reynold, Prandtl number and nozzle target spacing $(\frac{z}{d})$. It is true that the experimental arrangement for constant wall temperature boundary condition, in order to determine the heat transfer coefficient is difficult, hence current work, tries to propose a unique form of a varying heat flux. Such exponentially varying heat flux boundary condition and its inverse are some of the similar keens of constant temperature boundary conditions.

The objective of the current study is to establish and correlate the slope (m) of non-uniform heat flux, input velocity, nozzle –target spacing and heat transfer rate. The computations were performed using SST-K omega turbulence. In the later part the article proposes few empirical correlation, correlating the Nusselt number with $Re, \frac{z}{d}$ and slope (m). Local Nusselt profile r/d is the local parameter incorporate.

2. NUMERICAL METHODOLOGY

2. 1. Computational Approches The computational domain as shown in Figure 1 consist of flexible nozzle target spacing $(2 < \frac{z}{d} < 6)$. Exponentially varying heat flux boundary condition is implemented for heating purpose. The numerical simulations are carried out using fluent and SST-K omega as solver and primary turbulence model, respectively. The Reynolds Number varies between 2000 to 14000 . Katti and Prabhu [4], proposed the correlation for Nusselt number magnitude for Reynolds number range 12000 to 28000.

The impingement was carried out, using straight smooth nozzle of 7.35 mm diameter. Sajad et. al. [17], proposed the stagnation Nusselt number correlation for Reynolds number range of $6000 - 14000$. The air impinging nozzle was 13 mm in diameter and $L = 32D$. The diameter of impinging nozzle is selective, since the present study classifies the stagnation $(\frac{r}{d} \leq 0)$, transition $\left(1 < \frac{r}{d} > 2.5\right)$ and wall jet region $\left(\frac{r}{d} > 2.5\right)$, separately.

The present study is carried out for the range of impinging Reynolds number, $2000 - 14000$ under impinging nozzle of 8 mm. The air velocity at exit of the nozzle at inlet temperature ranges from 2 m/s to 15 m/s (For the current range of Reynolds number) The velocity of air is calculated using $Re = \frac{\rho V d}{\mu}$ .The air velocity ranges from $2\ m/s$ to $15\ m/s$. The nozzle diameter is chosen as $8\ mm$ (4). The nozzle target spacing z/d varies between $2 - 6$.

$$Q = Q_0 \times e^{mx} \quad (1)$$

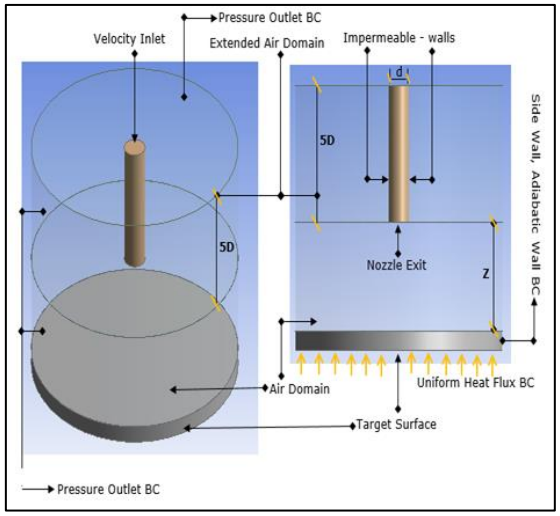

Figure 1. Computational Domain

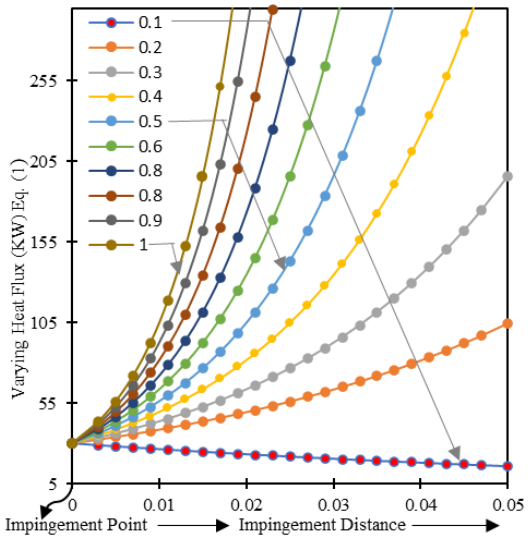

Figure 2. Exponential Varying Heat Flux condition

The heat flux boundary condition that changes exponentially from the stagnation point to far end region of the plate is mapped in Figure 2. Equation 1 defines the boundary condition as a ramping heat flux input, and Q_0 denotes the constant heat flux magnitude, m represents the slope of exponentially varying heat flux. The heat transfer rate for a fully developed impingement causes a forced convection. The heat transfer rate for forced convection is given in Equation 2 (16).

$$Q = h\, A_s\, (\bar{T}_s - \bar{T}_f) \tag{2}$$

The governing equation for Continuity , momentum and the energy are solved simultaneously in ANSYS FLUENT by using second order upwind method. The value of turbulence intensity at nozzle exit is set to 1-3% and turbulence Prandtl number as 0.7 (22).

$$\frac{\partial u_i}{dx_i} = 0 \tag{3}$$

$$\frac{\partial(\partial u)}{\partial t} + \rho u_j \frac{\partial u_i}{\partial x_j} = -\frac{\partial p}{\partial x_i} + \frac{\partial}{\partial x_j}(2\mu S_{ij} - \rho\overline{u'_\iota u'_j} \tag{4}$$

$$\frac{\rho(\partial T)}{\partial t} + \rho u_j \frac{\partial T}{\partial x_j} = \frac{\partial}{\partial x_j}(\frac{k}{C_p}\frac{\partial T}{\partial x_j} - \overline{\rho u'_\iota T}) \tag{5}$$

where, S_{ij} is mean strain rate and C_p, μ & k are specific heat, viscosity and Thermal conductivity. Shear Stress Transport model, combining the effect of free stream and near wall region, gave satisfactory results for constant Heat Flux and Constant Temperature Boundary Condition. The four-equation turbulence model equation of SST and $Gamma - Theta$ is summarized with Equation.

$$\frac{\partial k}{\partial t} + U_j \frac{\partial k}{\partial x_j} = P_k - \beta * k\omega + \partial/\partial x_j[\left[\frac{(\vartheta + \sigma_k \vartheta_t)\partial k}{\partial x_j}\right] \tag{6}$$

$$\frac{\partial \omega}{\partial t} + U_j \frac{\partial \omega}{\partial x_j} = \alpha S^2 - \beta\omega^2 + \partial/\partial x_j[\left[\frac{(\vartheta + \sigma_w \vartheta_t)\partial w}{\partial x_j}\right] + 2(1 - F_1)\sigma_{w2}\, \frac{1}{\omega}\frac{\partial k}{\partial xi}\, \frac{\partial \omega}{\partial xi} \tag{7}$$

In Equations 6 & 7 k represents the turbulent kinetic energy and ω represents the specific dissipation rate. $(\vartheta + \sigma_k \vartheta_t)$ and $(\vartheta + \sigma_w \vartheta_t)$ represents the effective diffusivities of k and ω respectively. αS^2 is cross diffusion term. Sajad Alimohammadi et al. (17) validated the SST and transition $Gama - Theta$ turbulence model, with CFX solver. Zhang et al. (32) validated the use of $SST\ K - Omega$ turbulence model for constant Heat Flux Boundary Condition. The computation time with use of $SST + K$ −Omega was found to be far less (60%), as compared with CFX (22).

2. 2. Grid Independence Test An adaptive mesh with different growth rate along X and Y axis are generated using Mesh modeler of Ansys pack 2023R1. Growth rate are kept adaptive, in order to generated optimal number of nodes and cell size. The mesh shown in Figure 3, is orthogonal unstructured, with skewness in range of 0.9-1 The heat transfer highly relies on quality and density of grid and number of nodes and structure of computational domain. Hence, to ensure that the grid independence result and optimistic time of computation. Grid independence is carried out by varying the number of nodes of 2-D computational domain. The grid independence is carried out at $\frac{z}{d} = 4$ & $Re = 12000$. The distance of first cell from wall, in combination with post computing multiple, defines a non-dimensional y^+. As per Nikuradse (33), this value is maintained much less than 1, throughout the domain. Figure 4 shows the Nusselt number distribution for various grid sizes.

In order to get optimum grid size, number of divisions are varied along the radial and axial directions, ranging from 240 to 480 and 280 to 520, respectively. However, it is advisable to adjust the number of divisions according

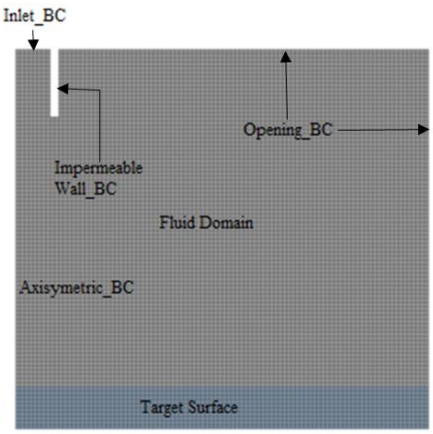

Figure 3. Schematic diagram of grid

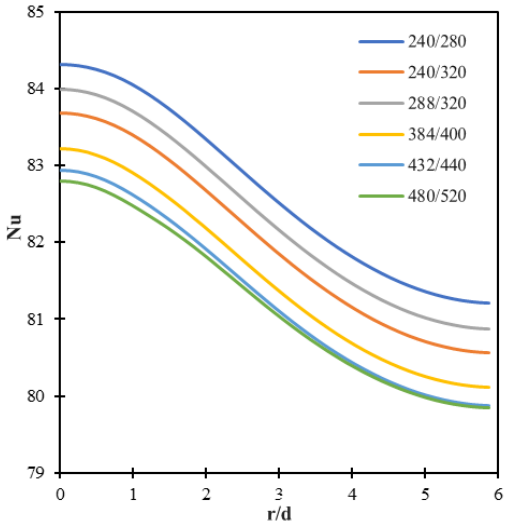

Figure 4. Nusselt profile for various number of division over radial/axial direction at z/d=4 & Re=12000

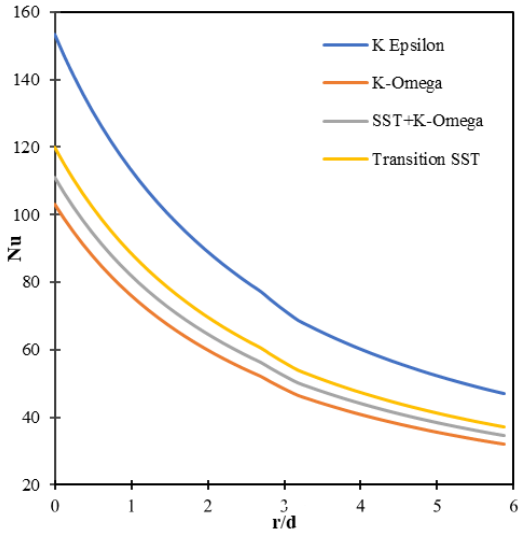

Figure 5. Nusselt profile for different Turbulence Models at z/d=4 & Re=12000

to changes in the $(\frac{z}{d})$ value.Thus, mesh size containing 480 the number of divisions on radial and 520 number of division on axial edge is found to give the results within $\pm 1\%$ of previous grid size.

2. 3. Validation of Turbulence Model As per the literature study, especially for impingement of jet, it is very crucial to accurately compute the heat transfer in both the near wall and far wall regions, which majorly dependence on the choice of appropriate turbulence model. A graphical comparative study is carried out at $\frac{z}{d} = 4$ and Reynolds number 12000. Figure 5 illustrates the result of heat transfer, in form of Nusselt profile for different turbulence model. The adverse pressure gradient effect makes the $k-$epsilon turbulence model fails to predict the heat transfer. On the other hand, the $k-$omega turbulence model provides an accurate profile but deviates significantly, In near jet and far jet region. This is due its especially in predicting the flow behavior in near wall region for 'Internal Forced Convection'. The discrepancy arises for the model choice and its ability to predict turbulence vortices generated, due to impingement. Menter (34) strongly justifies the use of SST turbulence model for estimating turbulence heat transfer with air jet. The SST turbulence model ncorporates an additional term that effectively predicts the production and termination of local turbulence vortices, the turbulence production term (p_k). Not only that the latest study by Alimohammadi et al. (17) and Umair et al. (35) strongly recommend the use of SST-K omega and SST-Gamma Theta for accurately mapping the turbulence behavior for the case of impingement. The current work is inclined towards measurement of heat transfer for ranges of Reynolds number (Re), nozzle target spacing $\left(\frac{z}{d}\right)$ and slope parameter (m) against radial distance $(\frac{r}{d})$. Figures 6(a) & 6(b) represent the validation of current grid size and turbulence model with the results of Katti and Prabhu (4). The proposed correlation at stagnation $\left(0 < \frac{r}{d} < 1\right)$ and transition region $\left(1 < \frac{r}{d} < 2.5\right)$, digitized and compared in Figures $7(a)$ & $7(b)$. Validations are carried out for $\frac{z}{d} = 4$ and Reynolds number of 10000,12000 and 14000 which are shown in Figures $6(a)$ & $6(b)$. The approximate percentage error of present computation with Katti and Prabhu (4) results lies within $\pm 10\% \sim \pm 15\%$. The underestimation of heat transfer results with FLUENT, as in present case, is due to the lack of constraints in mapping the turbulence vortices and its timely changed behavior with different boundary condition.

2. 4. Overall and Local Cooling Rate for Different Reynolds Number Figure 7 shows the Nusselt number magnitude distribution with varying Reynold number at constant nozzle target spacing of 4 and slope of 0.5. In the present study Reynolds number is varied from $2000 - 14000$. With an increase in Reynolds number the local Nusselt magnitude increases along, locally. The average Nusselt magnitude increases with an increase in Reynolds number. The stagnation increase is due to the adverse pressure gradient and radial increase is due to higher velocity gradient. At higher velocity, the heat carried away quickly and thus forced convection renders better heat transfer coefficient, with impingement.

2. 5. Overall and Local Cooling Rate for Different Nozzle Target Spacing (z/d) Figure 8 represents

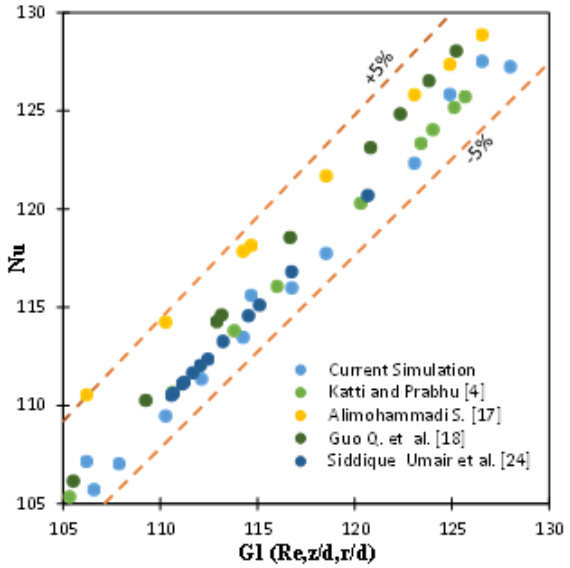

(a) Stagnation Region

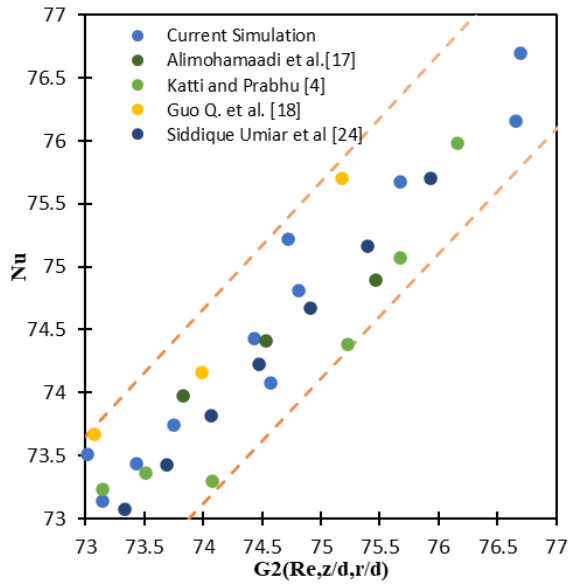

(b) Transition Region

Figure 6 (a) & (b). Turbulence model validation at stagnation and transition region

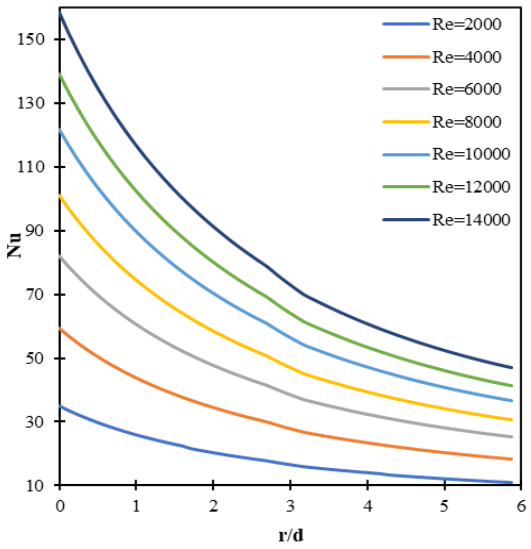

Figure 7. Nusselt Profile at different Reynold number

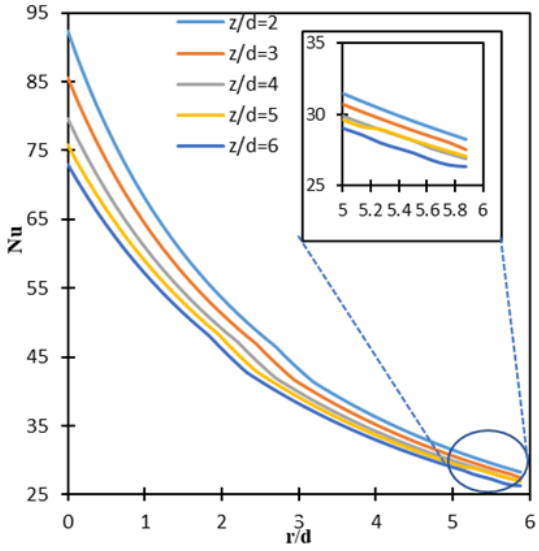

Figure 8. Nusselt profile at varying z/d

the variation of nozzle target spacing $\left(\frac{z}{d}\right)$ at a constant Reynold number of 12000. The Nusselt profile exhibit a consistent slope value of 0.5. As the distance between nozzle and target surface increases, the local Nusselt magnitude decrease. However, this trend is not applicable for a nozzle target spacing less than 1 $\left(\frac{z}{d} < 1\right)$. This is due to the under- development of the potential core and lack of computational model availability. At a Reynold number of 12000, the potential core is well developed for nozzle target spacing values greater than 4 resulting a smooth Nusselt profile.

2. 6. Overall and Local Cooling Rate for Different Slope of Varying Heat Flux Figure 9 represents the Nusselt profile with a Reynold number of 12000 and z/d=4 at various slope (m) parameter of Input heat flux. The observation from Figure 9 indicate the heat dissipation to be more at lower slope $(m < 0.5 - 0.6)$. The heat transfer rate from the impinging fluid to the target surface reduces as the slope of heat flux increases. The local Nusselt number is reduced for higher slopes of heat input, and the overall distribution of the Nusselt profile under non-uniformity heat flux boundary conditions is Affected. Such non-uniformity is of practical importance in electronic packaging system.

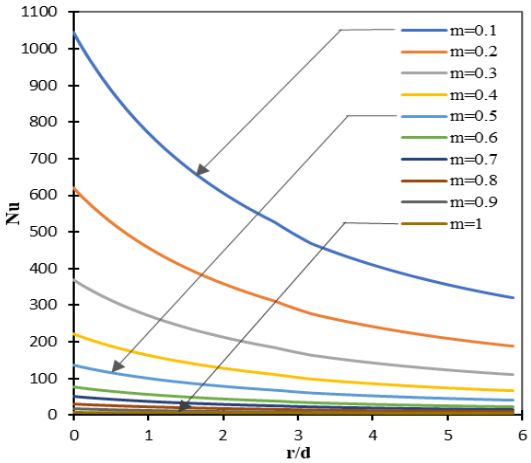

Figure 9. Nusselt Profile at different slope of input

2. 7. Semi-empirical Correlations Representing Nusselt Profile In the current simulation the Nusselt number empirical relation is proposed for various regions at stagnation region ($\frac{r}{d}=0$) & ($0<\frac{r}{d}<1$), transition region (1<r/d<2.5) and wall jet regions ($\frac{r}{d}>2.5$). The empirical correlations are formed using regression analysis by sampling the data of different heat transfer results of varying Reynolds (Re), $\frac{z}{d}$ & m. Table 1 shows the corresponding correlation for every individual region. The correlations proposed in Table 1, is within $\pm 15\%$ error, and should be applicable for practical problems of non-uniform heat flux. The error of $\pm 15\%$ as shown in Figure 10 is well in line with external forced convection of , Cenjal (16).

TABLE 1. Proposed Correlation for Local Nusselt Number at Different Regions

Region	Function	Semi-empirical relation
Stagnation region ($\frac{r}{d}=0$)	$G1\left(\mathrm{Re},\frac{z}{d},m,\frac{r}{d}\right)$	$Nu=0.0282\times(Re)^{0.815}\left(\frac{z}{d}\right)^{-0.131}(m)^{-1.425}$
Stagnation region ($0<\frac{r}{d}<1$)	$G2\left(\mathrm{Re},\frac{z}{d},m,\frac{r}{d}\right)$	$Nu=0.0212\times(Re)^{0.815}\left(\frac{z}{d}\right)^{-0.104}(m)^{-1.419}\left(\frac{r}{d}\right)^{-0.119}$
Transition region ($1<\frac{r}{d}<2.5$)	$G3\left(\mathrm{Re},\frac{z}{d},m,\frac{r}{d}\right)$	$Nu=0.0254\times(Re)^{0.788}\left(\frac{z}{d}\right)^{-0.078}(m)^{-1.419}\left(\frac{r}{d}\right)^{-0.382}$
Wall jet region ($\frac{r}{d}>2.5$)	$G4\left(\mathrm{Re},\frac{z}{d},m,\frac{r}{d}\right)$	$Nu=0.192\times(Re)^{0.79}\left(\frac{z}{d}\right)^{-0.202}(m)^{-1.328}\left(\frac{r}{d}\right)^{-0.584}$

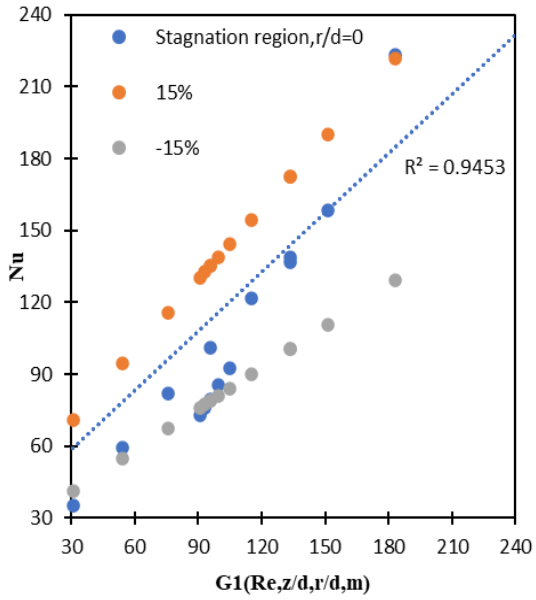

(a)

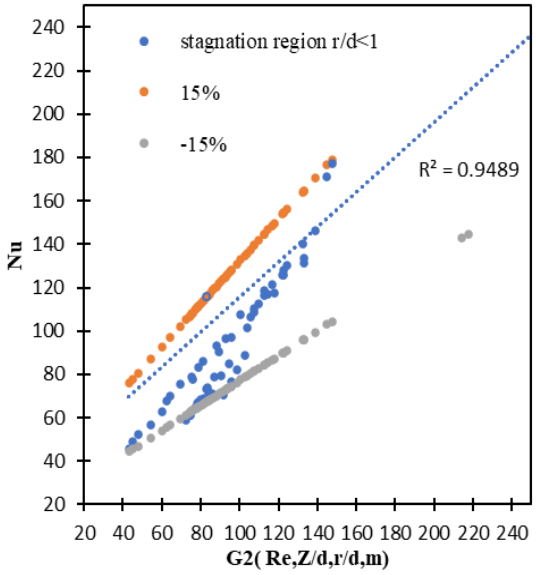

(b)

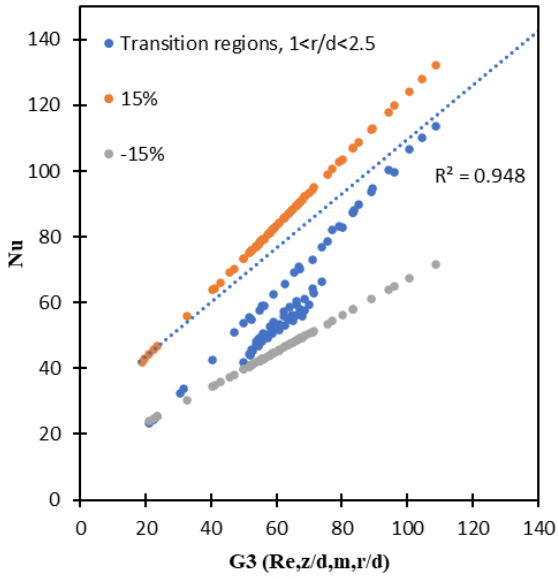

(c)

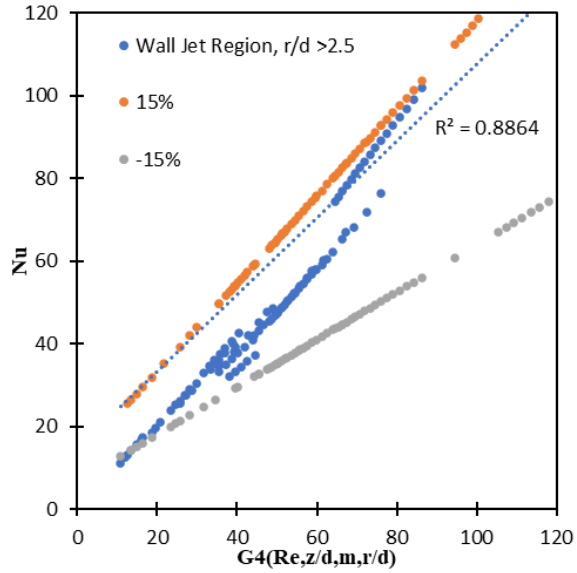

(d)

Figure 10. Validation of G1, G2, G3 &G4 function with local Nusselt number

3. CONCLUSION

The present work investigated using exponentially varying heat flux boundary, inevitably justifies the dependency of impinging Reynolds number (pumping power) and nozzle-target surface spacing, as that of constant heat flux boundary condition literature. The extended robustness of SST coupled K-Omega turbulence model in computing the flow field for non-uniform boundary condition is observed. The local cooling profile (Nu Vs G (Re, z/d, m, r/d)) for non-uniform exponent of 0.1 – 1, is found to replicate the constant wall temperature boundary condition. The customized exponentially powered heat flux boundary condition can be taken as the substitute for constant wall temperature boundary condition computation purpose. Many commercial computing software like FLUENT, OpenFOAM, MATLAB. is less responsive to such constant wall temperature boundary condition.

4. SCOPE OF FUTURE WORK

Constant wall temperature boundary condition is seamless problem for young researchers, specially when it is simulation in FLUENT. As per the most authorative textbooks, the constant wall temperature boundary condition, is achieved with wall hot water circulation. Such traditional arrangement in FLUENT, will require extra computational effort and time. The novel exponentially powered heat flux boundary condition renders a similar result as that of constant temperature. The choice of exponent magnitude, as per the available non – uniform heat flux or uniform temperature, can be easily replicated with exponent magnitude. The generic profile of exponential heat flux boundary condition can be further investigated more to its equivalency for constant temperature BC. The exponential slope parameter can even be use for defining the cooling in various material processing industries, to forecast the type of strength desired.

5. ACKNOWLEDGMENTS

The experimental setup received financial support from Technical Education Quality Improvement Program-II (TEQIP-II/MH2G03/204)/778) at Veermata Jijabai Technological Institute under the guidance of Prof. N P Gulhane. Prof. Nitin P Gulhane is currently acting as a supervisor and Dr. Siddique Umair is the co-supervisor. Mr. Avinash–M. Rathod (First Author) has received Research Fellowship for investigating Jet Impingement Heat Transfer from Mahatma Jyotiba Phule Research & Training Institute (MAHAJYOTI-Fellowship 2022_198).

6. REFERENCES

1. Ricou FP, Spalding D. Measurements of entrainment by axisymmetrical turbulent jets. Journal of fluid mechanics. 1961;11(1):21-32. https://doi.org/10.1017/S0022112061000834
2. Hoogendoorn C. The effect of turbulence on heat transfer at a stagnation point. International Journal of Heat and Mass Transfer. 1977;20(12):1333-8. https://doi.org/10.1016/0017-9310(77)90029-1
3. Pamadi B, Belov I. A note on the heat transfer characteristics of circular impinging jet. International Journal of Heat and Mass Transfer. 1980;23(6):783-7. https://doi.org/https://doi.org/10.1016/0017-9310(80)90032-0

4. Katti V, Prabhu S. Experimental study and theoretical analysis of local heat transfer distribution between smooth flat surface and impinging air jet from a circular straight pipe nozzle. International Journal of Heat and Mass Transfer. 2008;51(17-18):4480-95. https://doi.org/10.1016/j.ijheatmasstransfer.2007.12.024
5. KATAOKA K, SHUNDOH H, MATSUO H. A generalized model of the development of nonisothermal, axisymmetric free jets. Journal of Chemical Engineering of Japan. 1982;15(1):17-22. https://doi.org/DOI:10.1252/JCEJ.15.17
6. Behera RC, Dutta P, Srinivasan K. Numerical study of interrupted impinging jets for cooling of electronics. IEEE Transactions on Components and Packaging Technologies. 2007;30(2):275-84. https://doi.org/10.1109/TCAPT.2007.898353
7. Shadlesky P. Stagnation point heat transfer for jet impingement to a plane surface. AIAA Journal. 1983;21(8):1214-5. https://doi.org/10.2514/3.8231
8. Hollworth B, Gero L. Entrainment effects on impingement heat transfer: part II—local heat transfer measurements. 1985. https://doi.org/https://doi.org/10.1115/1.3247520
9. Zumbrunnen D, Incropera F, Viskanta R. Convective heat transfer distributions on a plate cooled by planar water jets. 1989. https://doi.org/https://doi.org/10.1115/1.3250802
10. Goldstein R, Seol W. Heat transfer to a row of impinging circular air jets including the effect of entrainment. International journal of heat and mass transfer. 1991;34(8):2133-47. https://doi.org/https://doi.org/10.1016/0017-9310(91)90223-2
11. Lytle D, Webb B. Air jet impingement heat transfer at low nozzle-plate spacings. International Journal of Heat and Mass Transfer. 1994;37(12):1687-97. https://doi.org/10.1016/0017-9310(94)90059-0
12. Behnia M, Parneix S, Shabany Y, Durbin P. Numerical study of turbulent heat transfer in confined and unconfined impinging jets. International Journal of Heat and Fluid Flow. 1999;20(1):1-9. https://doi.org/https://doi.org/10.1016/S0142-727X(98)10040-1
13. Garimella SV, Schroeder VP. Local heat transfer distributions in confined multiple air jet impingement. J Electron Packag. 2001;123(3):165-72. https://doi.org/10.1115/1.1371923
14. Han B, Goldstein RJ. Jet-impingement heat transfer in gas turbine systems. Annals of the New York Academy of Sciences. 2001;934(1):147-61. https://doi.org/https://doi.org/10.1111/j.1749-6632.2001.tb05849.x
15. Sagot B, Antonini G, Christgen A, Buron F. Jet impingement heat transfer on a flat plate at a constant wall temperature. International Journal of Thermal Sciences. 2008;47(12):1610-9. https://doi.org/10.1016/j.ijthermalsci.2007.10.020
16. Çengel YA, Ghajar AJ. Heat and Mass Transfer: Fundamentals [and] Applications: McGraw-Hill Education; 2020.
17. Alimohammadi S, Murray DB, Persoons T. Experimental validation of a computational fluid dynamics methodology for transitional flow heat transfer characteristics of a steady impinging jet. Journal of Heat Transfer. 2014;136(9):091703. https://doi.org/10.1016/j.ijheatmasstransfer.2016.09.048
18. Guo Q, Wen Z, Dou R. Experimental and numerical study on the transient heat-transfer characteristics of circular air-jet impingement on a flat plate. International Journal of Heat and Mass Transfer. 2017;104:1177-88. https://doi.org/10.1016/j.ijheatmasstransfer.2017.03.064
19. Luhar S, Sarkar D, Jain A. Steady state and transient analytical modeling of non-uniform convective cooling of a microprocessor chip due to jet impingement. International Journal of Heat and Mass Transfer. 2017;110:768-77. https://doi.org/10.5829/idosi.ije.2015.28.10a.14
20. Muniyandi V. Heat transfer study of perforated fin under forced convection. International Journal of Engineering, Transactions A: Basics,. 2015;28(10):1500-6. https://doi.org/10.5829/idosi.ije.2015.28.10a.14
21. GULHANE N, Siddique U. On numerical investigation of non-dimensional constant representing the occurrence of secondary peaks in the Nusselt distribution curves. International Journal of Engineering, Transactions A: Basics,. 2016;29(10):1431-40. https://doi.org/10.5829/idosi.ije.2016.29.10a.00
22. Mohd Umair S, Gulhane N, Al-Robaian A, Khan SA. On numerical investigation of semi-empirical relations representing local nusselt number at lower nozzle-target spacing's. International Journal of Engineering, Transactions A: Basics,. 2019;32(1):137-45. https://doi.org/10.5829/ije.2019.32.01a.18
23. Umair SM, Gulhane NP. On numerical investigation of nonuniformity in cooling characteristic for different materials of target surfaces being exposed to impingement of air jet. International Journal of Modeling, Simulation, and Scientific Computing. 2017;8(03):1750024. https://doi.org/10.1142/S1793962317500246
24. Siddique UM, Bhise GA, Gulhane NP. On numerical investigation of local Nusselt distribution between flat surface and impinging air jet from straight circular nozzle and power law correlations generation. Heat Transfer—Asian Research. 2018;47(1):126-49. https://doi.org/10.1002/htj.21295
25. Siddique Mohd U, Ansari E, Khan SA, Gulhane NP, Patil R. Numerical Investigation of Nondimensional Constant and Empirical Relation Representing Nusselt Profile Nonuniformity. Journal of Thermophysics and Heat Transfer. 2020;34(1):215-29. https://doi.org/10.2514/1.T5828
26. Husain A, Ariz M. Thermal performance of jet impingement with spent flow management. International Journal of Engineering, Transactions A: Basics,. 2017;30(10):1599-608. https://doi.org/10.5829/ije.2017.30.10a.22
27. Aminzadeh M, Khadem J, Zolfaghari S, Omidvar A. Numerical Investigation on Oscillation Behavior of a Non-isothermal Self-excited Jet in a Cavity: The Effects of Reynolds Number and Temperature Differences. International Journal of Engineering, Transactions C: Aspects. 2022;35(6):1193-201.
28. Manglik R, Prusa J. Viscous dissipation in non-Newtonian flows-Implications for Nusselt number. Journal of thermophysics and heat transfer. 1995;9(4):733-42. https://doi.org/10.2514/3.732
29. Lu G, Cheng P. Friction factor and Nusselt number for thermoacoustic transport phenomena in a tube. Journal of thermophysics and heat transfer. 2000;14(4):566-73. https://doi.org/10.2514/2.6558
30. Wang X, Bibeau E, Naterer G. Experimental correlation of forced convection heat transfer from a NACA airfoil. Experimental thermal and fluid science. 2007;31(8):1073-82. https://doi.org/10.1016/j.expthermflusci.2006.11.008
31. Wang X, Naterer G, Bibeau E. Multiphase Nusselt Correlation for the Impinging Droplet Heat Flux from a NACA Airfoil. Journal of thermophysics and heat transfer. 2008;22(2):219-26. https://doi.org/10.2514/1.32401
32. Zhang Y, Li P, Xie Y. Numerical investigation of heat transfer characteristics of impinging synthetic jets with different waveforms. International Journal of Heat and Mass Transfer. 2018;125:1017-27. https://doi.org/10.1016/j.ijheatmasstransfer.2018.04.120
33. Williamson J. The laws of flow in rough pipes. La Houille Blanche. 1951(5):738-57. https://doi.org/10.1051/lhb/1951058
34. Menter FR. Influence of freestream values on k-omega turbulence model predictions. AIAA journal. 1992;30(6):1657-9. https://doi.org/10.2514/3.11115
35. Umair SM, Kolawale AR, Bhise GA, Gulhane NP. On numerical heat transfer characteristic study of flat surface subjected to variation in geometric thickness. International Journal of Computational Materials Science and Engineering. 2017;6(02):1750010. https://doi.org/10.1142/S2047684117500105

Persian Abstract

چکیده

سرعت خنک کننده تحت برخورد جت هوا کاربرد گسترده ای در بسته بندی الکترونیکی، صنایع پردازش مواد و خنک سازی توربین گاز پیدا می کند. خنک سازی معمولی سینک های حرارتی تا به امروز با استفاده از فن و پمپ انجام می شد. اخیراً مشخص شده است که برخورد مهم هوا در مقایسه با روش معمولی، ۱.۵ برابر سرعت خنک‌سازی با قدرت پمپاژ یکسان تولید می‌کند. پیش از این، تحقیقات جذابی در مورد مشاهده سرعت خنک‌سازی برای شرایط مرزی شار حرارتی ثابت انجام شده است و کمتر برای دمای ثابت دیوار در دسترس است. تحقیق حاضر یک بررسی عددی عمیق را برای چنین سینک های حرارتی برخورد شده با جت، با شرایط مرزی شار حرارتی ارائه می دهد. تغییر نمایی بزرگی شار حرارتی با فاصله شعاعی (دور از نقطه برخورد)، به عنوان یک جایگزین عمومی از شرایط مرزی دمای دیواره ثابت مشاهده می‌شود. محاسبات عددی برای انتقال حرارت چنین سینک شار حرارتی با نیروی نمایی با استفاده از FLUENT (ANSYS 2023R1) انجام می‌شود. یک دامنه محاسباتی مش دوبعدی متعامد با مدل تلاطم SST و K-Omega فشرده برای سرعت ورودی و فاصله نازل-هدف مختلف شبیه‌سازی شده است. برخورد جت و خنک کننده موضعی سطح هدف به ترتیب با استفاده از عدد رینولدز و ناسلت غیربعدی شناخته شده تعریف می شود. توان نمایی برای سینک‌هایی که به طور یکنواخت گرم می‌شوند را می‌توان به آسانی انتخاب کرد (۰.۱-۱) برای تکرار گرمایش غیریکنواخت فعلی یا شرایط مرزی دمای دیوار ثابت. گرمایش غیریکنواخت توجه بسیاری از محققین انتقال حرارت را در سراسر جهان به خود جلب کرده است. نتایج محاسباتی استخراج‌شده برای عدد رینولدز مختلف و فاصله نازل-هدف، با استفاده از رگرسیون بهترین برازش را داشتند و با نتایج ادبیات قبلی ارجاع شده اعتبارسنجی شدند. وابستگی شدید پارامتر شیب به عدد رینولدز و z/d در نرخ خنک‌سازی موضعی مشاهده می‌شود. این وابستگی ها بر اساس قدرت توان ها قضاوت می شوند. همبستگی های نیمه تجربی به طور جداگانه برای مناطق رکود، انتقال و جت دیواری به طور جداگانه تعریف می شوند. چنین همبستگی می تواند طراحی سیستم خنک کننده را در شرایط گرمایش غیر یکنواخت برنامه ریزی کند.